Chinese Chemical Letters 32 (2021) 168–178

Contents lists available at ScienceDirect

Chinese Chemical Letters

journal homepage: www.elsevier.com/locate/cclet

Review

Recent advances in the development of activatable multifunctional probes for *in vivo* imaging of caspase-3

Pengzhan Wang[a,1], Huocheng Yang[b,c,1], Chang Liu[b,c,1], Mingqiang Qiu[c,*], Xin Ma[d], Zhiqiang Mao[a,*], Yao Sun[c,*], Zhihong Liu[a]

[a] *Hubei Collaborative Innovation Center for Advanced Organic Chemical Materials, Ministry of Education Key Laboratory for the Synthesis and Application of Organic Functional Molecules & College of Chemistry and Chemical Engineering, Hubei University, Wuhan 430062, China*
[b] *State Key Laboratory of Pathogenesis, Prevention and Treatment of High Incidence Diseases in Central Asia, Xinjiang Medical University, Xinjiang 830011, China*
[c] *International Joint Research Center for Intelligent Biosensor Technology and Health, Key Laboratory of Pesticides and Chemical Biology, Ministry of Education, College of Chemistry, Central China Normal University, Wuhan 430079, China*
[d] *State Key Laboratory of Elemento-Organic Chemistry, Nankai University, Tianjin 300071, China*

ARTICLE INFO

Article history:
Received 28 September 2020
Received in revised form 23 November 2020
Accepted 24 November 2020
Available online 30 November 2020

Keywords:
Fluorescence imaging
Multi-functional
Activatable probe
Caspase-3

ABSTRACT

Caspases are a family of proteases that play critical roles in controlling inflammation and cell death. Apoptosis is a caspase-3 mainly controlled behavior to avoid inflammation and damage to surrounding cells, whereas anomalistic cell apoptosis may be associated with many diseases. The detection and imaging of caspase-3 will be of great significance in evaluating the early therapeutic effect of tumors. Developing smart fluorescent probes may be helpful for the visualization of therapeutic effect compared with "always on" probes. Thus, more and more works toward activatable fluorescent probes for caspase-3 imaging have been reported. In addition, multifunctional probes have also been designed to further improve the imaging of caspase-3. Herein, this review systematically summarized the representative work of caspase-3 from the perspective of molecular design that it will play a guiding role in the design of probes that respond to caspase-3. Also, challenges and perspectives toward the field for imaging of cell apoptosis (caspase-3) are also discussed.

1. Introduction

Apoptosis refers to the autonomous and orderly process of cell death controlled by genes to maintain the stability of the internal environment [1]. It involves the activation, expression, and regulation of a series of genes including Bcl-2 family, Caspase family, oncogene, *etc*. Among these various genes, Caspase family is a protein system that directly leads to the disintegration of apoptotic cells and plays an important role in maintaining homeostasis [2,3]. Because the Caspase family proteases have two major characteristics of cysteine proteases and specific aspartate sites, they are also called Caspase proteases.

Up to now, 14 kinds of Caspases have been discovered and most of them are apoptotic initiators or effectors [4–6]. According to the distinctive functions during the cascade reaction in the whole process of apoptosis, Caspases can be broadly divided into 3 categories: (1) Caspases existing as initiators usually include caspase-2, caspase-8, caspase-9, caspase-10. Especially for caspase-8 and caspase-9, they exist as inactive procaspase monomers and can self-activate with the participation of other proteins and activate downstream caspases; (2) Caspases existing as effectors includes caspase-3, caspase-6, caspase-7. As for downstream of the cascade reaction, caspase including caspase-3, caspase-6, caspase-7 can be activated by upstream initiators and act on specific substrates to cause cells to undergo biochemical and morphological changes, thus leading to apoptosis; (3) Caspases that are mainly involved in cytokine-mediated inflammatory response and play an auxiliary role in the apoptosis pathway mediated by death receptors. Such as, caspase-1, caspase-4, caspase-5, caspase-12 [7]. Although so many types of caspases have been discovered, caspase-3 is the only one that has been thoroughly studied so far. Once caspase-3 is activated, it will make the apoptosis process inevitable so that it is also called death protease. Moreover, caspase-3 is the main downstream effector caspase that cleaves the majority of the cellular substrates in apoptotic cells [8,9].

* Corresponding authors.
E-mail addresses: qiumingqiang@mail.ccnu.edu.cn (M. Qiu), maozq@hubu.edu.cn (Z. Mao), sunyaogbasp@mail.ccnu.edu.cn (Y. Sun).
[1] These authors contributed equally to this work.

https://doi.org/10.1016/j.cclet.2020.11.056

As an important executive protein, caspase-3 initially is inactive in cells [10–13]. With the early state of the apoptosis process, caspase-3 has been activated and cleaved itself under the action of caspase-8, 9 and 10, then it forms an active enzyme which has ability to cleave proteins [14–16]. What followed is to break the DNA of the chromosome, then lead to damage of nuclear and the formation of apoptotic bodies [17]. Therefore, caspase-3 usually acts as a biomarker of apoptosis that could reflect the efficacy of therapeutic for tumor in time to screen out a more effective treatment to improve the survival rate of cancer patients.

Not only an important role of caspase-3 plays in the process of apoptosis, it also involved in the process of pyroptosis, a new form of programmed cell death (PCD) accompanied by the release of a large number of pro-inflammatory factors [18–21]. Compared with apoptosis, pyroptosis occurs faster. The traditional cell pyroptosis pathway is activated by caspase-1 which can cleave gasdermin D (GSDMD) into the N-terminal and C-terminal [21,22]. Then, the N-terminal section will cause cell membrane perforation and further induce a series of cascade reactions including recruiting inflammatory factors to cause inflammatory death of cells [23–27]. A recent report indicated that gasdermin E (GSDME) and GSDMD have a 28% similar region [28], which can be specifically cleaved by caspase-3 to induce pyroptosis by releasing N-terminal. Thus, caspase-3 can also be used as a promoter of cell pyroptosis [28,29]. However, the content of GSDME in most cancer cells is much lower than that of normal cells [30–33].

Therefore, understanding the activity of caspase-3 is crucial provide a guidance for further cancer treatment. Moreover, anomalistic cell apoptosis may be associated with many diseases. During several past decades. Many researchers have made great contributions in this field, such as Rao, Ye and Liang *etc*. [34,35]. The visualization of caspase-3 is what researchers have pursued in the past few decades. Up to now, there are many imaging modalities for *in vivo* imaging of caspase-3 such as positron emission computed tomography (PET) [36–38]/magnetic resonance imaging(MRI) [39–45]/fluorescence (FL) *etc*. [46,47]. Among them, fluorescence has the advantages of intuitive, non-invasive, non-radiative, low-cost, and real-time imaging that it has been widely used [48,49]. In recent years, research staff has combined fluorophore with caspase-3 responsive sites to construct a series of probes for evaluating the therapeutic efficacy and exploring the transformation between apoptosis and pyroptosis.

At present, although many published reviews provide a summary of enzyme-activated probes, reviews focusing on the enzyme caspase-3 are still rare [50,51]. Herein, this review summarized the representative work of caspase-3 from the perspective of molecular design that it will play a guiding role in the design of probes that respond to caspase-3. It can be seen that the development of probes has a tendency to develop from a single responsive site to multi-responsive sites in this review. Last but not least, challenges and perspectives toward the imaging of caspase-3 are also discussed.

2. Single responsive for construction of "turn-on" fluorescence probes

2.1. Probes combined with multiple quenching methods

Generally, most organic fluorescent probes for imaging caspase-3 are designed based on the signal from "OFF" to "ON". Therefore, it is important to quench the fluorescence before the activation of caspase-3. The earlier organic fluorescent probes used for caspase-3 imaging are usually based on förster resonance energy transfer (FRET). Moreover, aggregation-caused quenching (ACQ) and intramolecular charge transfer (ICT) are applied in quenching fluorescence. These quenching methods will be introduced separately below.

2.1.1. Förster resonance energy transfer (FRET)

DEVD (Asp-Glu-Val-Asp) is the most commonly used peptide substrate to be specifically hydrolyzed by caspase-3 [52]. Kwon *et al.* conjugated a DEVD linked near-infrared fluorescent dye Cy5.5 and branched poly(ethyleneimine) (PEI) backbone modified with amphiphilic deoxycholic acid (DOCA) to synthesize a self-quenching polymeric nanoprobe, Cy5.5-$DEVD_{26}$-PEI-$DOCA_{20}$ [53]. Due to the ACQ effect, the fluorescence of Cy5.5 in the polymer nanoparticles was quenched. In the presence of caspase-3/7, Cy5.5 was released from the polymer nanoparticles with the hydrolysis of the DEVD peptide chain, and the fluorescence was enhanced to image the caspase-3/7 in real-time toward TNF-related apoptosis-inducing ligand (TRAIL)-treated HeLa cells.

However, self-quenching probes cannot effectively reduce the interference from background signal that the method based on FRET is considered to be a more promising way to image caspase-3 proteases. FRET is a mechanism describing distance-dependent energy-transfer between two molecules. Owing to the overlaps between emission spectrum of the donor moiety and the absorption spectrum of the acceptor, an electronically excited donor molecule transfers its energy *via* a nonradiative dipole–dipole coupling to a ground-state acceptor molecule when the spatial distance of the two molecules is within 10 nm, thus it will be observed that the fluorescence of donor decreases while the fluorescence of acceptor increases [54].

Responsive detection for caspase-3 controlled by the integrity of DEVD is easily to realize when utilizing the process of FRET between the fluorophore and the quencher. The energy transfer between the fluorophore and the quencher leads to the fluorescence quenching. When the DEVD chain is hydrolyzed by caspase-3, the fluorophore shows an enhanced fluorescence signal. Piwnica-Worms and co-workers linked AlexaFluor 647 (the fluorophore) and QSY21 (the quencher) to the two terminals of a peptide containing DEVD fragment. Further, a cell-penetrating peptide based on a sequence of Ac-RKKRRORRR [55] was incorporated into the structure to improve the ability of cell membrane penetration to obtain a fluorescent probe TcapQ647 (Fig. 1a). The far-red fluorescence signal from AlexaFluor 647 of the probe could be turned on under caspase-3/7 activation to achieve fluorescence imaging at the cellular and *in vivo* levels [56,57]. Afterward, the group changed the original arginine-rich cell-penetrating peptide sequence to lysine-rich Ac-KKKRKV to obtain new probes KcapQ [58]. This change resulted in KcapQ having a higher quenching efficiency and lower cytotoxicity than that of TcapQ647.

Sometimes, traditional "turn-on" probes have almost no signals after being activated by caspase-3, and the main reasons are attributed to the weak caspase-3 activity, insufficient probe concentration and improper probe cellular localization. Therefore, detecting the ability of fluorescent substrates to enter the cells would be of great significance in biology. Wagner *et al.* reported a FRET-based probe CDQ-DEVD-G-DEAC, in which 4-hydroxy-2-metoxy-phenylazo benzoic acid was a chemically deactivatable quencher (CDQ), 7-diethylamino-coumarin-3-carboxylic acid (DEAC) was a fluorescent dye [59]. The fluorescence of such probe could be turned on by responding to an enzyme or a chemical reagent (sodium dithionite). Under the activation of caspase-3, the fluorescence signal could be recovered to some extent with the hydrolysis of the DEVD chain of parts of probes.

Moreover, the azo groups in CDQ could react readily and under mild reduction conditions with dithionite. Consequently, residual probes which not hydrolyzed by caspase-3 can further increased the fluorescence through deactivating the quencher by dithionite

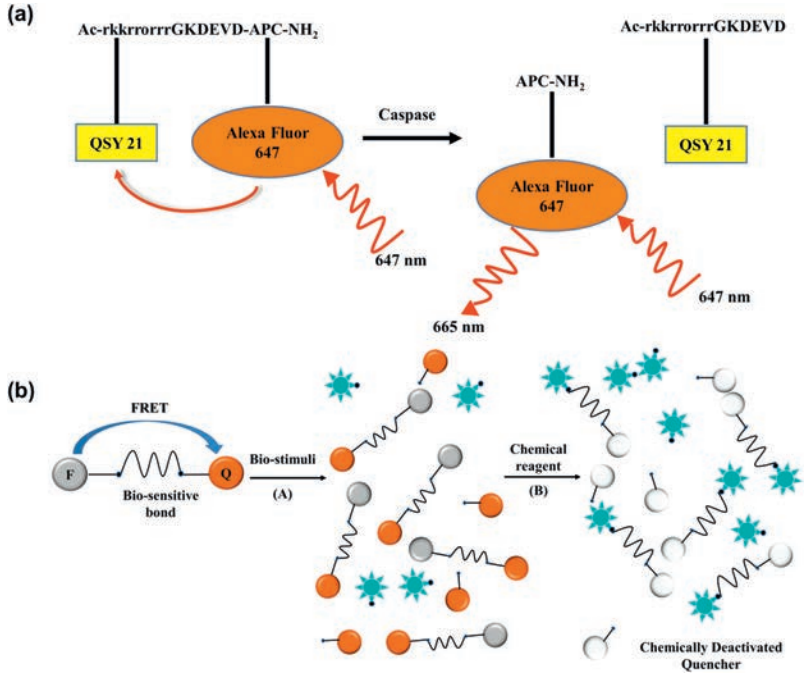

Fig. 1. (a) Schematic diagram of imaging caspase with activatable fluorescent probe TcapQ647. Reproduced with permission [55]. Copyright 2005, American Chemical Society. (b) Schematic diagram of the design principle of the FRET-based probe with a chemically deactivatable quencher. Reproduced with permission [59]. Copyright 2012, Royal Society of Chemistry.

(Fig. 1b). Therefore, the probe enabled us to calculate the total concentration and the conversion rate of the fluorescent substrates to quantify the caspase-3 responsive activity *in vitro*. Simultaneously, this novel strategy allowed us to reveal unreacted probes in cell conditions, thereby confirming the optimal incubation time between cells and probes, also controlling internalization and localization of the probe in living cells.

2.1.2. Combination of self-quenching and FRET

Compared with small molecule probes, nanoparticle-based probes have improved circulation time and numerous functional sites that can be used for further functionalization [60,61]. Thus, nanoparticles can provide a promising platform where more fluorophore-quencher energy transfer pairs can be attached to obtain nanoprobes for the detection of caspase-3. Owing to ACQ and FRET effects, nanoparticles-based fluorescent probes also present higher quenching efficiency and lower background signals [62].

Choi *et al.* developed a novel apoptosis nanoprobe (Apo-NP) through chemically conjugating NIR fluorogenic peptides (Cy5.5-Gly-DEVDAPKGC-BHQ-3) on the surface of hyaluronic acid-based polymeric nanoparticles (HA-NPs) [63]. Due to the efficient NIR fluorescence quenching ability of quencher Black Hole Quencher-3 (BHQ-3) based on FRET effect and self-quenching of the Cy5.5 dye based on ACQ, caspase-3-sensitive fluorogenic peptides were in a strongly dual-quenched state. The fluorogenic peptides were efficiently delivered into cells by the Apo-NP, and then cleaved by caspase-3. Therefore, the boosting fluorescence signals from Cy5.5 dyes were allowed to image caspase-3 activity in real-time toward apoptotic cells with a high resolution.

The nanoparticle-based probes always demonstrated the passive targeting capabilities due to enhanced permeability and retention (EPR) effect. Besides, nanoparticle-based probes could further conjugate with targeting moieties including antibodies or ligands to exhibit actively targeting ability, which further improved the signal-to-noise ratio for imaging. Jiang and co-workers designed and synthesized an effective FRET-based brain-targeted detection nanoprobe (DGLs-RVG29-FRET) for imaging apoptosis [64]. Such nanoprobe was constructed based on three parts: (1) a biodegradable synthetic polymer, dendrigraft poly-L-lysines (DGLs); (2) the brain-targeted peptide RVG29 (a rabies virus glycoprotein-derived peptide which can pass the blood-brain barrier through receptor-mediated transcytosis); (3) the caspase-3 cleavable peptide linker (DEVD) (Fig. 2a). The nanoprobe was successfully applied to detect caspase-3 in apoptotic neuron that provided opportunities for the early diagnosis of neurodegenerative diseases (Fig. 2b).

Previous studies indicated that gold nanoparticles (AuNPs) which can be used as effective energy acceptors have absorption spectra spanning a wide range, and it exhibit high quenching efficiency at a short distance of 1–5 nm from the fluorophore as donor [65–67]. Hence, FRET based nanoprobes constructed with gold nanoparticles as carriers have great potential for apoptosis imaging applications [68–70]. In the caspase-3 imaging nanosystem, gold nanoparticles play two roles: (1) the fluorescence quencher in the FRET system; (2) the carrier of the nanoprobe. Apoptosis imaging probes based on gold nanoparticles are usually simple, inexpensive, and efficient, and have great potential in biomedical applications.

Generally, apoptosis imaging probes have no therapeutic function. When the probes are used to image apoptotic tumor cells, it is usually necessary to treat the tumor with drugs in advance. Because the time interval between administration and imaging is difficult to control, sometimes the real-time imaging effect of caspase-3 is not ideal, leading to certain errors in the evaluation of drug efficacy. The development of apoptosis imaging probes with integration of diagnosis and treatment are expected to solve this problem. These probes can not only induce tumor apoptosis spontaneously, but also can reflect the specific conditions of apoptosis in real time, which have great biomedical value. Tang and co-workers combined the superior property of fluorescence quenching for AuNPs and the excellent catalytic activity of Fe_2O_3 to design and synthesize a bifunctional Au-Fe_2O_3 nanoparticles, RGD/FITC-DEVD-Au-Fe_2O_3 NPs [68]. The $\alpha_V\beta_3$

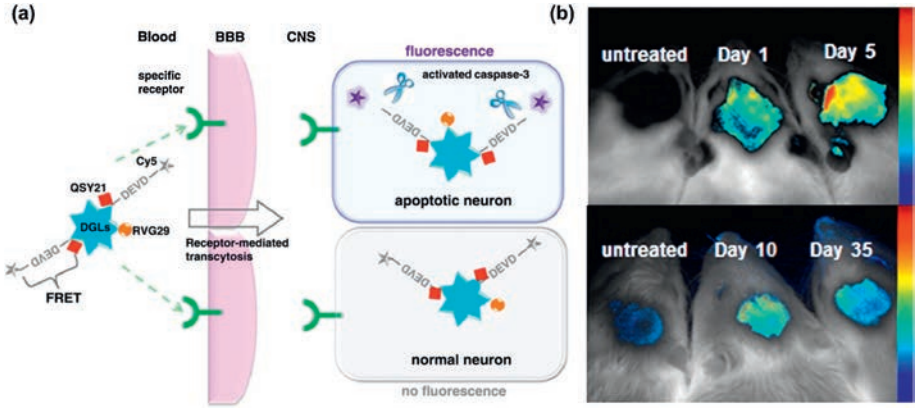

Fig. 2. (a) Schematic diagram of the brain-targeted DGLs-RVG29-FRET nano-device detecting caspase-3 of apoptotic neurons in central nervous system. (b) *In vivo* imaging after the intravenous injection of DGLs-RVG29-FRET with or without the treatment of rotenone on different days. Reproduced with permission [64]. Copyright 2012, Elsevier Ltd.

integrin-targeting peptide (RGD) on the Au surface could promote the probe to bind preferentially to integrin $\alpha_V\beta_3$-rich human liver cancer cells and initiate the catalytic formation of hydroxyl radical, and then enabled monitor the $^{\bullet}$OH-induced caspase-3-dependent apoptosis in real time by the responsive of fluorescein isothiocyanate (FITC)-labeled caspase-3 recognition sequence (DEVD) (Fig. 3a). Due to the polarization of the Au-Fe_2O_3 interface, the nanoprobe had excellent catalytic activity and thus had the functions of targeting, therapy and imaging.

In order to improve the sensitivity of detecting caspase-3, based on the large overlap between the emission of coumarin 343 (CM343) and the absorption of the AuNPs, which resulted in a high efficient energy transfer process between the donor and the acceptor in the whole system, Li and co-workers connected coumarin-functionalized AuNPs to polypeptide chains containing specific sequences (DEVD) to fabricate CM343-peptide@AuNP probes for the sensing of caspase-3 [69]. Caspase-3 cleaved the peptide-bridge and released CM343 from the AuNPs (quencher), which provided a basis for the detection of caspase-3 enzyme activity *in vitro*. The group also revealed that the shorter linker between the fluorophore and the AuNP quencher would result in a higher FRET efficiency and the recovery of emission would be more obvious after the linkage was cleaved by caspase-3. Therefore, the CM343-peptide 1@AuNP probe containing a shorter peptide chain had very high sensitivity, and the detection limit for caspase-3 was as low as 4 pg/mL.

The protein corona phenomenon is an obstacle to the use of nanoprobes for high-fidelity imaging *in vivo*. When nanoprobes are exposed to physiological environments (*e.g.*, blood), protein corona phenomenon usually changes the surface properties of the nanoprobe, such as reducing the delivery efficiency and targeting ability as well as bringing toxic side effects. Liu *et al.* encapsulated single nanoprobes (pep-AuNPs) in PEG-like multifunctional nanogels to prepare the probe AuNP@gel [70]. This multifunctional nanogel can shield the interaction between a single gold nanoparticle (AuNP) and serum protein under the combined effect from physical isolation of PEG-like cross-linking agent and the hydrophilic surface of zwitterionic monomer, thereby eliminating the formation of protein corona. When the probe entered the interest cell through endocytosis mediated by the folate receptor, the nanogel would degrade rapidly in the acidic endosome, and the ionizable monomer on the gel triggered the proton sponge effect, instantly transmitting Pep-AuNP to the cytoplasm (Fig. 3b). The fluorescence of Cy5 activated by caspase-3 enabled high-fidelity, non-invasive fluorescence imaging of caspase-3 in cancer cells and *in vivo* (Fig. 3c).

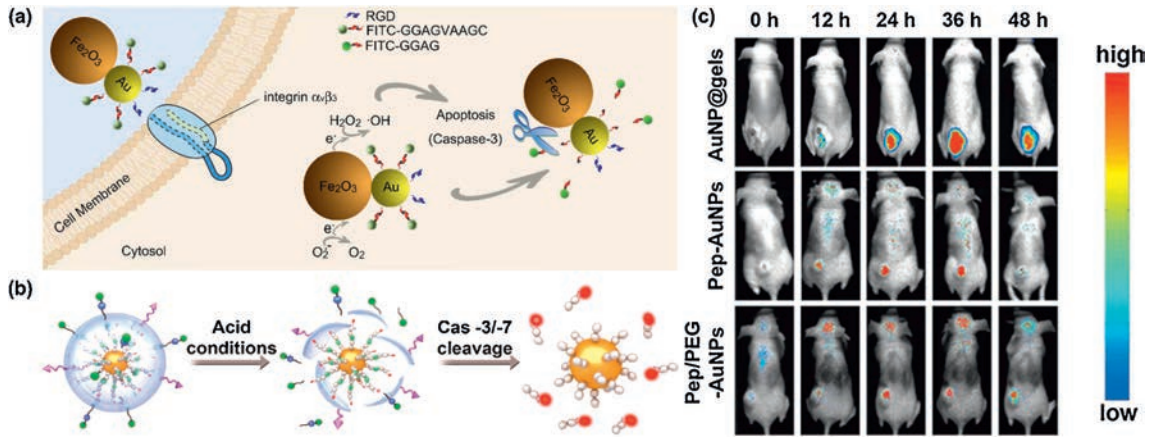

Fig. 3. (a) Schematic illustration of RGD/FITC-DEVD-Au-Fe_2O_3 NPs inducing cancer cell-specific apoptosis and the subsequent turning on fluorescent signal under caspase-3 cleavage. Reproduced with permission [68]. Copyright 2019, American Chemical Society. (b) schematic diagram of the acid degradation principle of the nanogel shell of AuNP@gel probe and the near infrared fluorescence imaging under the cleavage of caspase-3/7. (c) Fluorescent imaging of the tumor-bearing mice that were first administrated intravenously with AuNP@gel probes, Pep-AuNPs or Pep/PEG-AuNPs, respectively, and then treated with PBS or Doxorubicin (DOX) *via* intraperitoneal injection. The structure of Pep-AuNPs and Pep/PEG-AuNPs did not contain the multifunctional nanogel shells. Reproduced with permission [70]. Copyright 2019, American Chemical Society.

2.1.3. Intramolecular charge transfer

ICT mechanism is another detection mechanism widely used in the early development of fluorescent probes. It refers to the process of intramolecular charge transfer of molecules with push-pull electronic structure in the excited state, resulting in the separation of positive and negative charges in the molecule [71]. Generally, the ICT-activated fluorescent molecule probes are composed of a fluorophore and a recognition group. Moreover, the recognition group is an electron-withdrawing group. When it is connected to the donor of the fluorophore, it will cause blue-shift of the spectrum (Absorption/Emission (Abs/Em)) or quenching of fluorescence by weakening the push-pull electron ability for the molecule. After the recognition with the analyte, the recognition group will be removed to restore fluorescence [72,73].

Pu group reported a series of molecular probes (MRP1-3) with high renal clearance efficiency for *in vivo* optical imaging of drug-induced acute kidney injury (AKI) [74]. According to the report, the MRPs were very sensitive probes that detected AKI at the incipient stage, which was permitted longitudinal imaging of multiple biomarkers ($O_2^{\bullet-}$, the lysosomal enzyme *N*-acetyl-*β*-D-glucosaminidase (NAG) and caspase-3) in the kidneys of drug-treated living mice. Among MRP1-3, the near-infrared fluorescence of MRP3 was specifically activated by caspase-3 to image cellular apoptosis in the kidneys. The three probes constructed by three key building blocks: (1) a renal clearance moiety ((2-hydroxypropyl)-*β*-cyclodextrin (HP*β*CD), which could dramatically facilitate the removal of the probe by the kidney with an efficacy above 97%); (2) a biomarker reactive moiety (DEVD peptide sequence as the reactive moiety of caspase-3); (3) luminescent signal moiety (CyOH) (Figs. 4a and b). The MRPs were almost non-fluorescence at the intrinsic state, because they were 'caged' wherein the electron donating ability of the aromatic hydroxyl group was inhibited by the substituents. When the probes exposed to the biomarker and the response part subsequently was removed, the near infrared fluorescence signal could be turned from "OFF" to "ON". Then, the probes could almost be cleared by more than 80% ID (ID: injected doses) through the kidney at 3 h (Fig. 4c). The results of real-time imaging showed that oxidative stress, lysosomal damage and cellular apoptosis were prodromal molecular events occurring sequentially after nephrotoxic exposure (Fig. 4d). Meanwhile, the ability of MRPs to be used as urinalysis tracers to detect drug-induced AKI earlier than current assays further demonstrated their clinical promise for early diagnosis of AKI.

2.2. Probes combined with AIE

Most of traditional organic dyes are subjected to photobleaching and ACQ effects which limit further studies applications *in vivo*. Fortunately, Tang and co-workers discovered aggregation induced emission (AIE) effect opposite to ACQ in 2001 [75]. In solution, aromatic substituents in AIEgens freely rotate around a single bond and consume the energy of the excited state by non-radiation way, resulting in fluorescence quenching. On the contrary, the internal rotation of the molecule is greatly hindered due to the space limitation in the aggregation state, and the excited state can return to the ground state by the radiation path, leading to a significant increase in fluorescence. This is well known restriction of intramolecular rotation (RIR) mechanism [76]. Therefore, the AIE effects overcome the phenomenon of ACQ to a large extent. Recently, many organic luminogens with the property of AIE have been developed, which shows excellent performance in fluorescent light-up sensing and imaging with high signal-to-noise ratio.

Liu and Tang reported fluorescent light-up probe with live-cell-permeable, which could monitor apoptosis in real time and evaluate the efficacy of drugs [77]. In this work, the probe named Ac-DEVDK-TPE was composed of three components: hydrophilic caspase-3-specific recognition peptide Asp-Glu-Val-Asp (DEVD) peptide; tetraphenylethene (TPE) unit with regulating fluorescence off/on *via* external stimulation and the lysine as the linker to connect DEVD with and TPE units (Fig. 5a). In normal cell, the probe was almost non-fluorescent, while it displayed significant

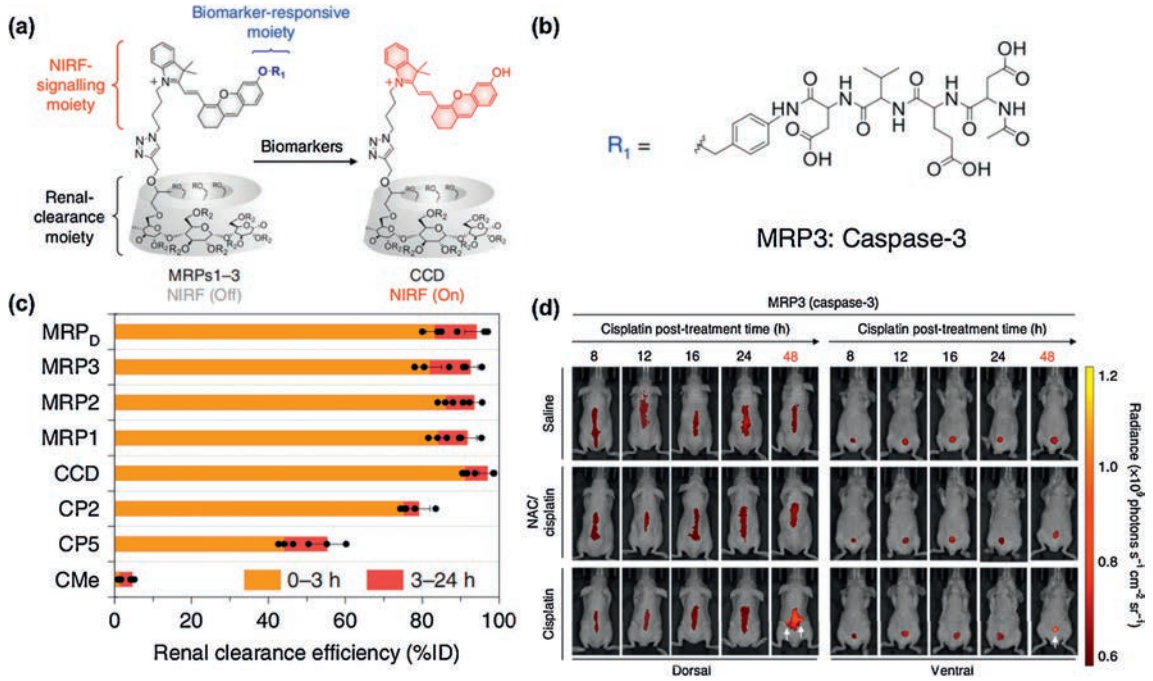

Fig. 4. (a) Chemical structures of MRP1-3 and (b) the activated form of MRP3 as HP*β*CD-substituted CyOH in response to caspase-3. (c) The renal clearance efficiency of MRPs and the uncaged fluorophores including CMe, CP2, CP5 and CCD at 0-3 h and 3-24 h after intravenous injection. (d) Fluorescence imaging of living mice at 8, 12, 16, 24 or 48 h after intravenous injection of MRP3. The white arrows indicate the kidneys in the dorsal side and bladder in the ventral side, respectively. Reproduced with permission [74]. Copyright 2019, Springer Nature.

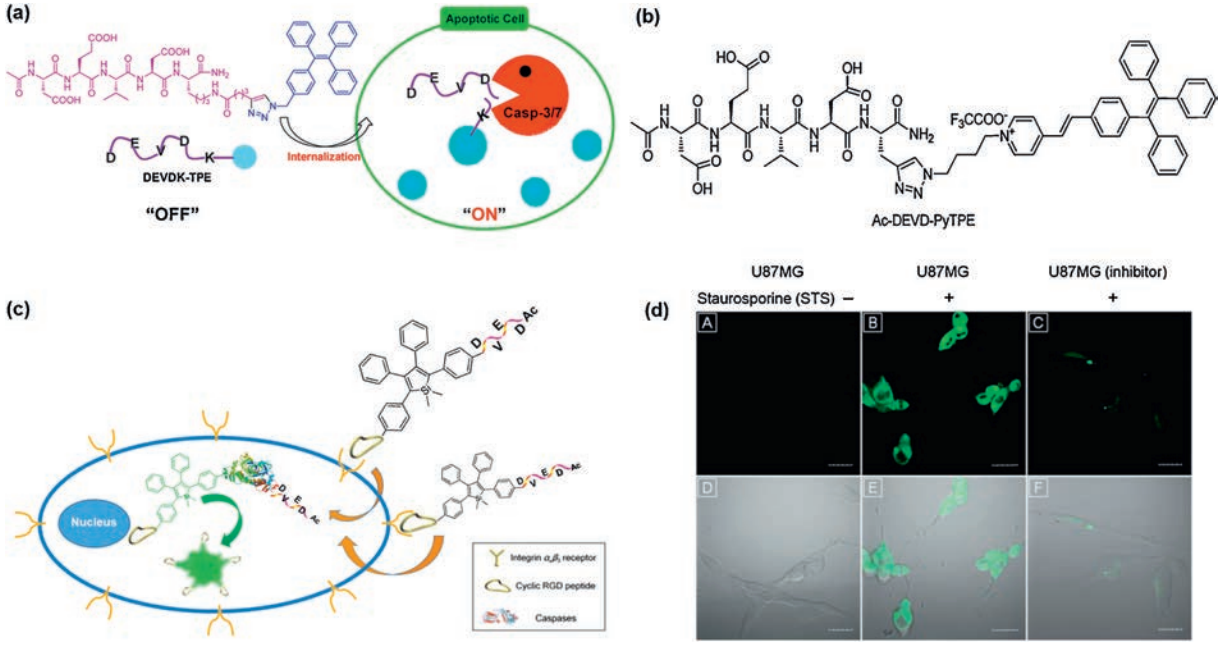

Fig. 5. (a) Schematic illustration of apoptosis imaging based on DEVDK-TPE. Reproduced with permission [77]. Copyright 2012, American Chemical Society. (b) Chemical structures of Ac-DEVD-PyTPE. (c) Schematic diagram of Ac-DEVD-TPS-cRGD targeted apoptotic imaging of tumor cells. (d) CLSM images of U87MG cells and MCF-7: (A) U87MG cells stained with Ac-DEVD-TPS-cRGD; (B) Staurosporine (STS)-induced U87MG cells and stained with Ac-DEVD-TPS-cRGD; (C) U87MG cells pretreated with STS and caspase inhibitors, and stained with Ac-DEVD-TPS-cRGD. The corresponding fluorescence/transmission merge images of (A–C) are (D–F), respectively. [Ac-DEVD-TPS-cRGD] = 5 mmol/L, [inhibitor] = 10 mmol/L, [STS] = 1 mmol/L. Scale bar: 30 mm. Reproduced with permission [79]. Copyright 2013, Royal Society of Chemistry.

fluorescence enhancement in apoptotic cells with high signal-to-noise ratios. The DEVD parts would be specifically cleaved by caspase-3/7, leading to the release of lysine-conjugated TPE (K-TPE). Due to K-TPE is hydrophobic, thus molecular aggregation would make fluorescence turn-on according to the AIE characteristic. Therefore, the strategy in this work provided an efficient platform for real-time imaging of live cell apoptosis, which could be *in situ* screening, quantification and evaluation of apoptosis-inducing agents (sodium ascorbate, cisplatin, and staurosporine (STS)). However, due to intrinsic photophysical property of TPE fluorogen with short wavelength emission, the wavelength of Ac-DEVDK-TPE limited *in vivo* studies. Fluorescent molecules with long wavelength absorption/emission and large stokes shifts can decrease the auto-fluorescence from bio-substrates *in vivo* imaging. Based on this point, Liu and Tang developed a new fluorescent light-up probe with AIE, Ac-DEVD-PyTPE [78], which was formed by conjugated between hydrophilic, targeting caspase-3/7 targeted Ac-DEVD peptide and hydrophobic azide-functionalized tetraphenylethene pyridinium (N3-PyTPE) fluorogen (Fig. 5b). In contrast to the Ac-DEVDK-TPE, Ac-DEVD-PyTPE increased conjugated length by adding pyridine group, and thus improving the wavelength of fluorescence emission (~470 nm *vs.* ~600 nm). The fluorescence of probe was quenched in solution; but the caspase-3 cleave DEVD, due to RIR, which increase energy *via* radiative channels, the AIE residues is emission, which can real-time monitor the caspase-3/7 activities *in vitro* and *in vivo*, screen tumors apoptotis-induced agents *in situ*. In addition, Liu and Tang designed fluorescent probe with AIE characteristic for real-time apoptosis imaging in target cancer cells [79]. The probe included three parts, acetyl protective N-terminal Asp-Glu-Val-Asp (Ac-DEVD), tetraphenylsilole (TPS) and cyclic Arg-Gly-Asp (cRGD) which showed high affinity to over-expressed integrin $\alpha_v\beta_3$ receptors in some cancer cells. In solution, fluorescence of the probe was off state (Fig. 5c). But when the caspase-3 cleaved Ac-DEVD, the fluorescence of resulted TPE-cRGD could turn on due to AIE characteristic. Furthermore, compared those aforementioned probes [77,78] without targeting peptide, the Ac-DEVD-TPE-cRGD had higher cell uptake and signal-to-noise ratio in living cell (Fig. 5d).

Moreover, to pursue sensitive fluorescent light-up probes with higher signal-to-noise ratio. Liu and co-works designed a highly sensitive AIE light-up probe by employing a short self-assembly peptide sequence GFFY [80]. When the TPE-GFFYK (DEVDEE -Ac) was cleaved by the caspase-3, the peptide GFFY could promote the ordered self-assembly of AIEgens to terrifically restrict the intramolecular motions of AIEgens, rendering the probes with high sensitivity (Fig. 6a). In contrast to TPE-K(DEVD-Ac) [77], the TPE-GFFYK-(DEVDEE-Ac) was cleaved by caspase-3 and the resulted TPE-GFFYK residues had higher signal-to-noise ratio due to the more orderly and regular arrangement of the molecule. Further, the space interaction between the molecules was closer and more compact, thus effectively limiting the intramolecular rotation of the benzene ring in TPE. In addition, compared to traditional FRET probes, which show single turn-on fluorescence signal upon responding to the analytes, Liu and co-workers developed the probe by AIEgen as the energy quencher, it is reported that this is the first probe that can react with the analyte to show a dual signal [81]. In this work, they designed a fluorescent probe, which is consisted of three parts, an AIEgen as the energy quencher, coumarin (Cou) as an energy donor and DEVD substrate for conjugation chain (Fig. 6b). The probe itself is non-emission, after the addition of caspase-3, Cou presented strong green fluorescence due to donor-acceptor separation. The released AIEgen residues aggregated that make made AIEgen to show a strong red fluorescence. Dual-signal activation can effectively monitor the activity of caspase-3 in living cells in real time for self-

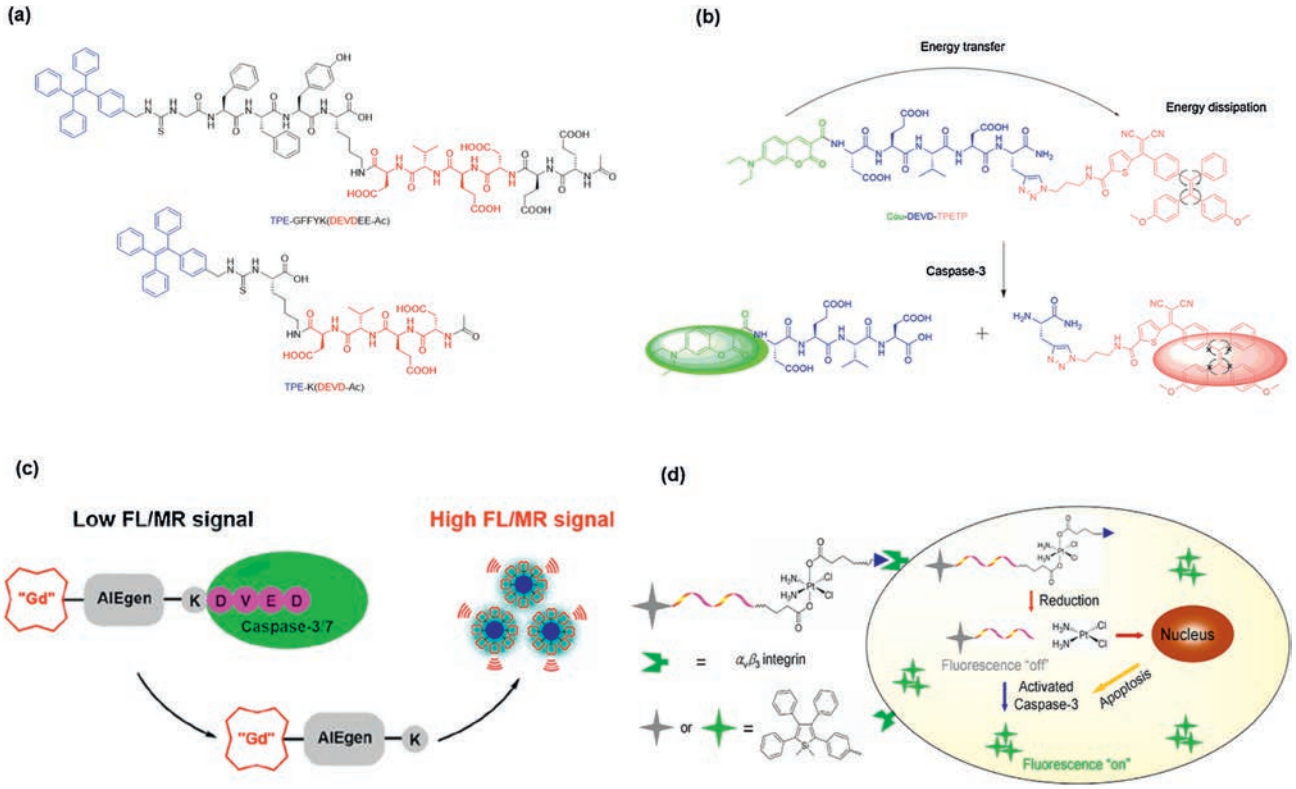

Fig. 6. (a) The structure of TPE-GFFYK(DEVDEE-Ac) and TPE-K(DEVDEE-Ac). Reproduced with permission [80]. Copyright 2012, American Chemical Society. (b) Schematic illustration of the FRET probe using AIEgen as energy quencher with dual signal output for self-validated caspase-3 detection. Reproduced with permission [81]. Copyright 2019, American Chemical Society. (c) Illustration of CP1 for caspase-3/7 activities study. (d) Schematic illustration of the theranostic Pt(IV) prodrug targeting an AIE fluorescence apoptotic sensor to evaluate non-invasive response to early treatment *in situ*. Reproduced with permission [83]. Copyright 2014, American Chemical Society.

validating enzyme detection and drug screening. Thomas. J. Meade and co-workers synthesized a dual-bimodal (FL/MR) caspase-activated imaging probe CP1 with bi-modal FL-MR, which was consisted of three parts, Gad, AIE and K-DEVD (Fig. 6c) [82]. Signal validation was a challenge for molecular imaging of bio-responsive MR probe, but the FL signal have good sensitivity, and confirm the MR signal enhancement in response to caspase-3. CP1 probe is cleaved by the caspase-3 and the residues shows higher MR/FL signal by aggregation. The probe exhibits FL-MR turn-on response in both *in vitro* caspase enzymatic assays and apoptotic HeLa cells. Most importantly, the FL signal of CP1 can be used to quantify the concentration of active and inactive probes in caspase-3 to accurately predict *in vitro* MR reactions.

Although most fluorescent probes with AIE characteristic have been designed for imaging cell apoptosis, these probes cannot report the exact location of the drug or the quantitative response to treatment, because the probe and drug may not be in the same cell, or the probe may not be co-localized with the drug when the probe and drug were in the same cell, it was highly desirable to develop a theranostic drug delivery system that can simultaneously assess treatment response. Therefore, Liu and Tang developed a targetable probe with cRGD (cyclic RGD) which could specifically bind with the over-expressed $\alpha_v\beta_3$ integrin in cancer cells, an apoptosis sensor (TPS-DEVD) with AIE characteristic, Pt(IV) prodrug which could slow down toxic side effects of Pt(II) caused by the distribution in normal tissues (Fig. 6d) [83]. The prodrug would preferentially target the integrin-overexpressed cancer cells to release prodrug Pt(IV), TPS-DEVD, and the prodrug Pt(IV) was further reduced to Pt(II) *in vivo* to exert its medicinal effects. Platinum(II) could induce apoptosis of cancer cells, and TPS-DEVD was cleaved by caspase-3 to recover the fluorescence that realize the integration of inducing apoptosis of cancer cells and monitoring apoptosis of cells in real time. The U87-MG cells apoptosis-induced emission spectral intensity have shown good correlation with the drug precursor concentration and cell viability, enabling rapid evaluation of the drug treatment response to guide treatment decisions (*e.g.*, whether the treatment is working well or should be discontinued).

3. Multi-responsive for functional imaging

3.1. Self-assemble

With the development of nanoscience and technology, the self-assembly process driven by hydrogen-bonding, π-π, hydrophobic interactions, *etc*., have received extensive attention from researchers [84–87]. The self-assembly system designed based on the tumor microenvironment stands out because of better specific response in the field of therapeutic evaluation. At the same time, the increase in the number of responsive sites can make the self-assembly process more controllable and precise. Therefore, Liang and coworkers designed a self-assemble and disassemble system for realizing sequential detections of glutathione (GSH) and caspase-3 in 2013 [88]. After entering tumor cells, disulfided cysteine motif could be reduced by overproduced GSH to expose the reactive group of 1,2-aminothiol. Then, the exposed reactive group could further react with cyano group of the 2-cyanobenzothiazole (CBT) motif. Thus, the self-assembly process can take place through this click chemistry and FITC-NPs could be formed. The caspase-3 responsive process reinforces the protonation of the double thiazoles group formed after self-assembly and subsequently make the FITC-NPs disassembled, further enhancing the

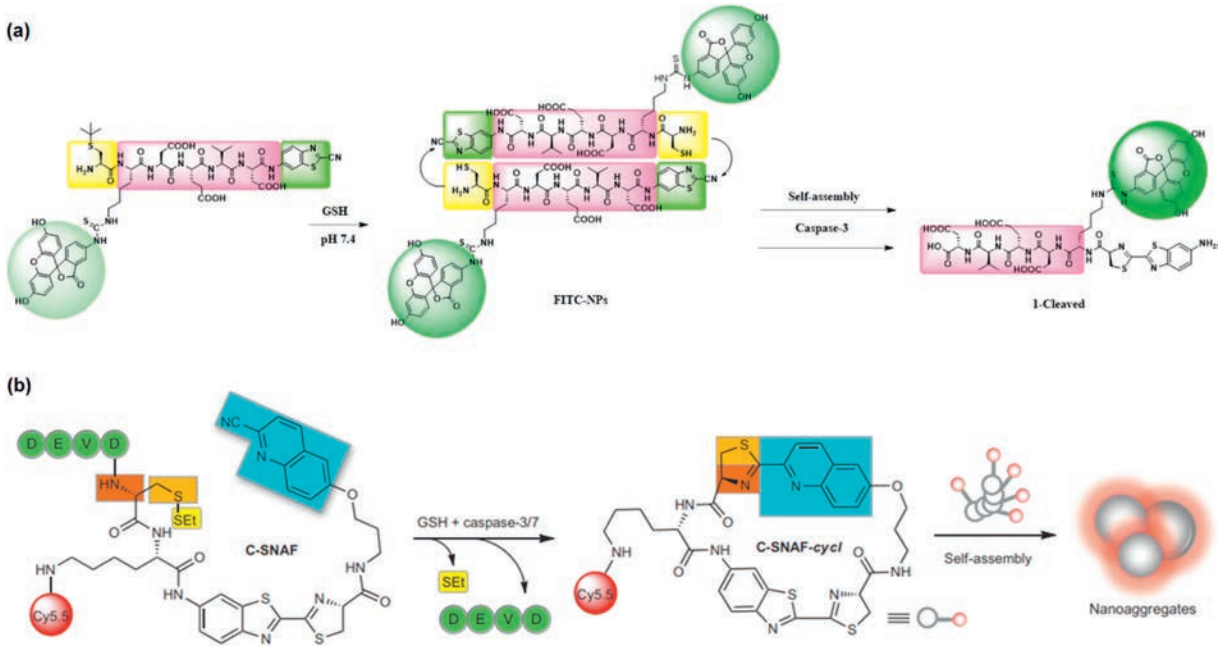

Fig. 7. (a) Schematic illustration of assembly/disassembly process of FITC-NPs controlled by GSH and caspase-3. Reproduced with permission [88]. Copyright 2013, American Chemical Society. (b) Schematic illustration of assembly process controlled by GSH and caspases (caspase-3/7). Reproduced with permission [89]. Copyright 2014, Nature Publishing Group.

fluorescence signal (Fig. 7a). This work combines click chemistry and self-assembly, which is of great significance for the subsequent scientific research. However, this work did not achieve detection in living organisms. By using similar design strategy, Rao and Ye *et al.* reported a probe and realized the imaging toward caspase activity *in vivo* [89]. Through the responsive of caspase-3/7 and GSH, the amino and thiol groups masked by DEVD and disulfide bonds are released to further react with cyano group of 2-cyano-6-hydroxyquinoline (CHQ) moieties so that the self-assembly process could occur and promote nanoaggregation *in situ* (Fig. 7b). Then, the feasibility of imaging caspase activity was verified at the cellular and living levels, respectively. As a result, obvious fluorescence from Cy5.5 linked on the macrocyclization product could be observed in the STS-treated cells and the region of DOX-treated subcutaneous HeLa tumor. As an important enzyme for cell programmed death, the distribution of caspase-3 is not evenly throughout the whole tumor. Therefore, probes that can reflect the spatial distribution of caspase are needed.

Recently, Ye and coworkers reported a caspase-3 activatable photoacoustic probe 1-RGD based on the same self-assembly strategy [90]. The difference from the previous reported case is that the fluorescence of the attached dye (indocyanine green, ICG) will undergo ACQ after self-assembly and aggregation that the photoacoustic signal would turn on (Fig. 8a). By linking a CHQ as preclickable site, the D cysteine (D-Cys) residue was modified with DEVD as well as disulfide bonds to serve as recognition sites for caspase-3 and GSH at the other end. After interaction with overproduced GSH and active caspase-3, free D-Cys could

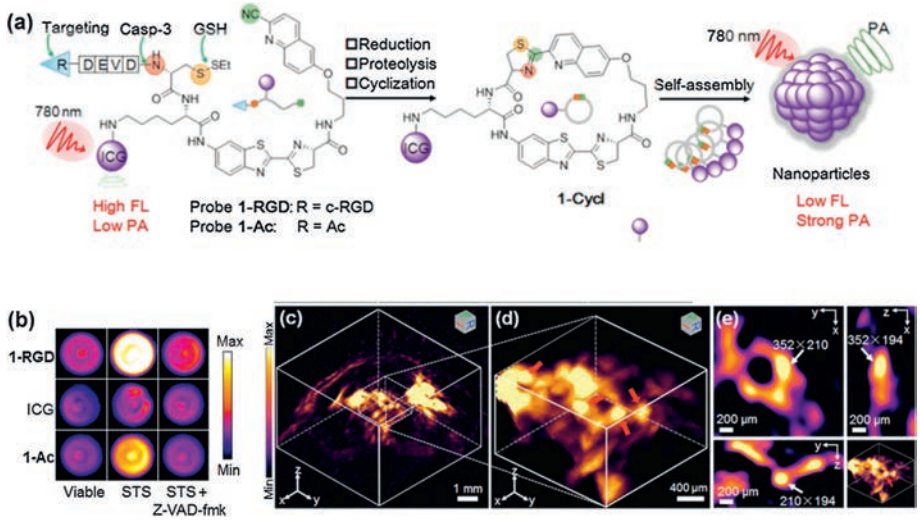

Fig. 8. (a) Schematic illustration of assembly/disassembly process of probe 1-RGD controlled by GSH and caspase-3. (b) PA images of apoptotic U87MG cells pretreated with viable, STS, Z-VAD-fmk (50 μmol/L) and subsequently incubated with 5 μmol/L 1-RGD, 1-Ac or ICG for 24 h. (c) 3D reconstruction PA image of tumor for DOX-treated mice after injected with 1-RGD for 10 h. (d) Enlarged 3D reconstruction PA image of the selected area in (c). (e) Enlarged 3D reconstruction PA image of 3D-slice in tumor tissues. Reproduced with permission [90]. Copyright 2019, Wiley-VCH.

subsequently condense with cyano of CHQ to form cyclized product 1-cycl. Owing to the aggregation of ICG, nonradiative relaxation process was enhanced that turn-on photoacoustic (PA) signal was observed. Benefiting from the superior penetration depth of PA imaging, high-resolution 3D images for the distribution of caspase-3 in entire apoptosis tumor tissues was obtained (Figs. 8b–e).

Because the exposed reaction sites can also cause intermolecular condensation reactions that reduce the occurrence of intramolecular cyclizatio, Rao and coworkers further explored the factors affecting cyclization by adjusting the substituents on aromatic nitriles as well as amino thiols and testing their reactivity, ability to form nanoparticles for cell imaging [91]. As a result, the reactivity of aromatic nitriles for their condensation with aminothiols was significantly affected by adding aromatic ring, electron-withdrawing substituents, and heteroatoms on the aromatic rings that further affects the rate of click chemistry. Moreover, changing the attached group on the cysteine residue can also recognize and image different kinds of enzymes. Therefore, more general imaging strategy toward various enzymes was explored and demonstrate a wider range of applications. Very recently, Rao and coworkers developed a pre-targeted imaging toward caspase-3 *in vivo via* the click chemistry reactions including the condensation reaction of aromatic nitriles and aminothiols, inverse-electron demand Deals-Alder reaction (IEDDA) between tetrazine and *trans*-cyclooctene (TCO) [92]. The constructed TCO-C-SNAT4 could be triggered macrocyclization and subsequent *in situ* self-assembly into nanoaggregates by caspase-3/7 *in vivo*. Then, Cy5-attached tetrazine was easily labeled to the TCO to imaging enzymatic activity. Due to the step-by-step targeting, excess fluorophores not used for imaging are rapidly metabolized. Moreover, TCO-C-SNAT4 can be repetitively injected to produce more TCO-nanoaggregates for click labeling to improve the retention of fluorescence signal of Cy5.

3.2. Multi-channel signals for imaging

For probes having multi-responsive sites, not only can self-assembly enhance signals, but also can be combined with other responsive sites to explore the relationship between other enzymes, cell apoptosis and evaluate therapeutic efficacy.

As is well-known, matrix metalloproteinase-2 (MMP-2) can break down extracellular matrix to facilitate the spread of tumor cells that plays an important role in tumor cell migration and invasion [93–96]. Moreover, the upregulation of MMP-2 would occur in some cancers such as melanomas [97,98], breast cancer [99], *etc*. Therefore, MMP-2 could usually act as a biomarker in tumor detection. Zhang *et al.* constructed a sequential responsive probe with two specific cleavable peptides, which can be specifically cleaved by MMP-2 and caspase-3, respectively. Initially, the fluorescence of this probe was quenched owing to FRET from 5(6)-carboxyfluorescein (FAM) to 4-{[4-(dimethylamino)-phenyl]-azo}-benzoic acid (Dabcyl). When this probe was treated with MMP-2 or caspase-3 for 10.5 h, the corresponding peptide was specifically cleaved. Hence, approximate 4.2-fold, 8.6-fold fluorescence enhancement could be observed in probe solutions while 16.6-fold fluorescence enhancement occurred after treated with MMP-2 and caspase-3 together for 10.5 h [100]. Based on the obvious change of fluorescence signal, this probe can perform effective sequential detection to MMP-2 and caspase-3. Thus, this probe can be applied to early apoptotic cell imaging induced by Dox/UV. However, owing to the sole emission at 520 nm after responding to MMP-2 or caspase-3, it is impossible to clearly and simultaneously image the spatiotemporal distribution of MMP-2 and caspase-3.

Afterwards, Zhang's group constructed a Mc-Probe based on multi-FRET, which was comprised of two specific peptides cleaved by MMP-2 and caspase-3 and three fluorophores. Among them, FAM served as the donor for both tetramethylrhodamine (TAMRA) and Dabcyl. Dabcyl was the acceptor for both FAM and TAMRA. When this probe arrived at the lesion location, the fluorescence was restored through cleaving peptides by corresponding enzymes that inhibited the process of FRET, and the process of multi-FRET would not be interfered with each other. Additionally, the fluorescence signals could be distinguished due to the different emission of FAM (520 nm) and TAMRA (570 nm), thereby collecting different fluorescent signals to clearly image the spatiotemporal distribution of MMP-2 and caspase-3 (Fig. 9a). When this probe was incubated with MMP-2 and caspase-3, the corresponding fluorescence signal could increase by 4.77 times and 45.99 times, respectively. Moreover, Mc-Probe was incubated with African green monkey fibroblast (COS7, normal cells) cells and squamous cell carcinoma (SCC-7, cancer cells, MMP-2 overexpression) cells for 6 h. As a result, bright red fluorescence for SCC-7 cells were able to be observed due to overproduced MMP-2. When the cells were treated by cisplatin for another 12 h, green fluorescence could be observed due to the reaction with caspase-3 in early apoptosis cells [101]. Therefore, Mc-Probe could be applied to realize the imaging of spatiotemporal distribution toward MMP-2 and caspase-3, which was beneficial to achieve precise disease diagnosis and evaluate therapeutic efficacy.

The construction of probes with multi-responsive sites is not only used for disease diagnosis, but also can be applied to explore the relationship between other enzymes and caspase-3 during the process of cell apoptosis. Liu and Tang *et al.* developed a turn-on probe composed of a hydrophilic peptide (DVEDIETD) and two fluorophores with AIE properties to understand the relationship between caspase-3 and caspase-8. This peptide contained specific responsive substrates for caspase-8 (IETD) and caspase-3 (DVED). Initially, the probe has almost no fluorescence in DMSO/PBS mixtures (1/99, v/v). Owing to hydrophilicity of the peptide, this probe was dissolved in the solution, the phenyl rings of the fluorophore could rotate freely. And the energy was attenuated in a non-radiative transition. After the probe incubated with caspase-3 or caspase-8, it could be observed that the fluorescence intensity gradually increased with the incubation time extended, which was attributed to the responsive of the peptide that the aggregation of fluorophore residues limited the rotation of the phenyl rings. Then, HeLa cells were incubated with the probe for 2 h and further treated with H_2O_2 to induce cell apoptosis that bright fluorescence could be observed [102], while the fluorescence generated by the responsive of caspase-8 is about 15 min earlier than caspase-3 (Fig. 9b). This probe could reveal the relationship between caspase-3 and caspase-8 in the cascade caspase activation during the process of H_2O_2-induced apoptosis. Moreover, the relationship between the activities of other different types of enzymes can be revealed through changing the sequences of peptide substrate.

To better understand the relationship between reactive oxygen species (ROS) and apoptosis, Yi and Xiao *et al.* designed a multicolor imaging probe (pep4-NP1) based on FRET. This probe was composed of NP1 (a reported H_2O_2-responsive dye [103]) and Cy5 (cyanine dye), wherein these two parts were linked by the caspase-3 specifically cleaved peptide SGDEVDSG. Originally, the probe had two absorption peaks at 555 nm and 663 nm under 450 nm excitation. After adding 500 μmol/L H_2O_2, the fluorescence intensity at 663 nm obviously increased while the fluorescence intensity at 550 nm slightly increased along with the treatment time. This phenomenon occurred due to the large spectral overlap between the emission peak of the 1,8-naphthalimide (donor) and the absorption peak of the Cy5 dye (acceptor), and energy transfer after laser excitation. However, in apoptotic HeLa cells, it could be observed that the intensity of green fluorescence increased significantly, while the red fluorescence increased slightly

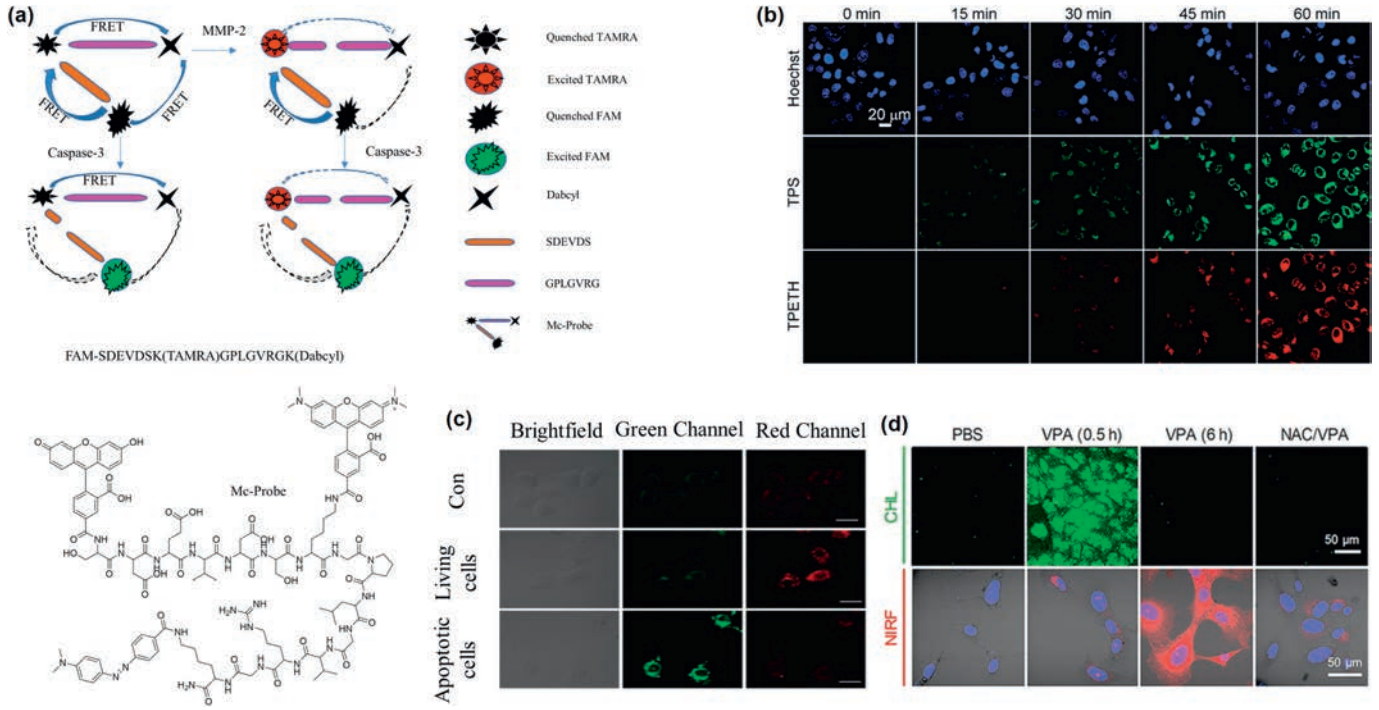

Fig. 9. (a) The construction strategy of Mc-Probe used for spatiotemporal imaging of MMP-2 and Caspase-3. Reproduced with permission [101]. Copyright 2017, American Chemical Society. (b) Confocal images of the probe **1** and HeLa cells incubated for 2 h and AIE residues images after treated with H_2O_2 for different time. Reproduced with permission [102]. Copyright 2017, Royal Society of Chemistry. (c) Confocal imaging of pep4-NP1-loaded HeLa cells and imaging of HeLa cells treated without and with H_2O_2. Reproduced with permission [104]. Copyright 2016, Elsevier Ltd. (d) Chemiluminescence and fluorescence signal images of mouse hepatocytes incubated with CFR probe and different pretreatments. Reproduced with permission [107]. Copyright 2019, American Chemical Society.

(Fig. 9c), which was attributed to the inhibition of the FRET process after DEVD cleaved by caspase-3 [104]. Therefore, this probe could simultaneously monitor the fluctuation of intracellular ROS and caspase-3 and determine whether the corresponding oxidative stress will cause apoptosis through the change of fluorescence.

In organisms, simultaneously monitoring toward multiple enzyme activities is very beneficial for disease diagnosis [105,106]. Although the previous work could monitor various enzymes at the same time, it was inevitable for spectral signal crosstalk in multicolor imaging, which affected the imaging resolution. Pu *et al.* designed a probe with no signal crosstalk to achieve accurate and sensitive imaging of superoxide anion ($O_2^{\bullet-}$) and caspase-3. The probe contained a responsive site for superoxide anion and a caspase-3 responsive site. Therefore, Pu *et al.* utilized this probe to detect drug-induced hepatotoxicity (DIH) and explored the relationship between oxidative stress and apoptosis. The signal generated by the superoxide anion of the probe after responding was chemiluminescence that it would not interfere with the imaging effect when the activities of superoxide anion and caspase-3 are simultaneously monitored. Moreover, the probe was incubated with mouse hepatocytes (AML-12), which were treated with valproic acid to trigger DIH. As a result, it could be observed that the signal generated from reaction with superoxide anion is earlier than the signal generated by caspase-3 (Fig. 9d). Therefore, it was confirmed that the superoxide anion was upregulated before the activation of caspase-3 [107]. This work tactfully introduced chemiluminescence, which solved the problem of spectral signal crosstalk in multi-color imaging.

4. Conclusions

In summary, the probes for detecting apoptosis signals have achieved great success in recent decades, which can not only evaluate therapeutic efficacy, but also reveal the relationship between other biologically active substances and apoptosis, such as other endogenous enzymes and reactive oxygen species. In this review, we mainly introduced the development process of "OFF" to "ON" fluorescent probes. First of all, for traditional enzyme response probes, it is very important to quench the original fluorescence of the probe to obtain a higher SBR. Here, we introduce a variety of fluorescence quenching methods to achieve better "OFF". In addition, in order to achieve a better "ON" process of fluorescence release, researchers now introduce AIE groups to enhance the fluorescence signal after DEVD cleaved. Furthermore, researchers are more focused on the field of multi-functional imaging at present. By introducing other active substance responsive sites to construct multi-channel signals responsive probes, further revealing the relationship between other active substances and cell apoptosis.

5. Perspective

1 Studies have shown that the concentration of caspase-3 is not uniform in different parts of the tumor, so it is of great significance to detect the spatial distribution of caspase-3 by optical imaging. Currently, PA imaging has been applied to detect the spatial distribution of caspase-3. However, compared with PA imaging, fluorescence imaging has higher sensitivity and can support the detection of low-concentration caspase-3 in some tumor sites. In addition, compared with near infrared-I and near infrared-II (NIR-I, NIR-II (1000–1700 nm)) fluorescence imaging has the characteristics of high spatial resolution, deep penetration and high signal-to-noise ratio. Therefore, it has great potential to develop NIR-II fluorescent imaging probes for the detection of caspase-3 spatial distribution.

2 As a new way of programmed cell death, the mechanism of pyroptosis remained unknown until 2015 when Shao and coworkers reported a new GSDMD protein. Compared with

apoptosis and necrosis, pyroptosis seems to be a promising way for tumor treatment. Developing a probe that can be used to detect pyroptosis will play an important role in drug screening for tumor. Until now, probes to detect pyroptosis are still in urgent need of development although there are some probes that can distinguish pyroptosis. Most of them are designed using peptides that respond to caspase-1, therefore, the method using peptide-based response maybe could be derived to design probes that respond to caspase-3 to reflect pyroptosis. Moreover, it is the expression level of GSDME that determines the form of cell death in caspase-3-activated cells. Therefore, combining a drug that induces an increase in GSDME content with a probe for caspase-3 detection seems to be a feasible attempt.

Declaration of competing interest

The authors report no declarations of interest.

Acknowledgments

This work was financially supported by the National Natural Science Foundation of China (Nos. 22074050, 22022404, 21804033), Wuhan Scientific and Technological Projects (No. 2019020701011441), Open Research Fund supported by the Key Laboratory of Pathogenesis, Prevention and Treatment of High Incidence Diseases in Central Asia Fund (No. SKL-HIDCA-2019-11), State Key Laboratory of Elemento-Organic Chemistry, Nankai University (No. 201901), the ministry of education Key laboratory for the Synthesis and Application of Organic Functional Molecules, Hubei University (No. KLSAOFM2011).

References

[1] M. Hengartner, Nature 407 (2000) 770–776.
[2] A. Ashkenazi, W. Fairbrother, J. Leverson, et al., Nat. Rev. Drug Discov. 16 (2017) 273–284.
[3] Y. Wang, R. An, Z. Lo, D. Ye, Chem. Eur. J. 24 (2018) 5707–5722.
[4] S. Kumar, Cell Death Differ. 14 (2007) 32–43.
[5] J.G. Walsh, S.P. Cullen, C. Sheridan, et al., Proc. Natl. Acad. Sci. U. S. A. 105 (2008) 12815–12819.
[6] A. Razgulin, N. Ma, J. Rao, Chem. Soc. Rev. 40 (2011) 4186–4216.
[7] A.G. Porter, R.U. Jänicke, Cell Death Differ. 6 (1999) 99–104.
[8] D. Ye, A.J. Shuhendler, L. Cui, et al., Nat. Chem. 6 (2014) 519–526.
[9] G. Condorelli, R. Roncarati, J.R Jr., et al., Proc. Natl. Acad. Sci. U. S. A. 98 (2001) 9977–9982.
[10] C. Buckley, D. Pilling, N. Henriquez, et al., Nature 397 (1999) 534–539.
[11] M. D'amelio, V. Cavallucci, F. Cecconi, Cell Death Differ. 17 (2010) 1104–1114.
[12] Y. Luo, J. Smith, V. Paramasivam, et al., Proc. Natl. Acad. Sci. U. S. A. 99 (2002) 12197–12202.
[13] C. Ma, Y. Zhang, Z. Jiao, et al., Chin. Chem. Lett. 31 (2020) 1635–1639.
[14] S.A. Lakhani, A. Masud, K. Kuida, et al., Science 311 (2006) 847–851.
[15] Y. Shaulov-Rotem, E. Merquiol, T. Weiss-Sadan, et al., Chem. Sci. 7 (2016) 1322–1337.
[16] J.T. Burgess, E. Bolderson, M.N. Adams, et al., Cell Death Dis. 7 (2016) e2469.
[17] J. Hannan, H. Matsui, N. Sopko, et al., Sci. Rep. 6 (2016) 29416.
[18] T. Bergsbaken, S.L. Fink, B.T. Cookson, Nat. Rev. Microbiol. 7 (2009) 99–109.
[19] J. Shi, W. Gao, F. Shao, Trends Biochem. Sci. 42 (2017) 245–254.
[20] X. Liu, Z. Zhang, J. Ruan, et al., Nature 535 (2016) 153–158.
[21] S.L. Fink, B.T. Cookson, Cell. Microbiol. 9 (2007) 2562–2570.
[22] G. Doitsh, N.L.K. Galloway, X. Geng, et al., Nature 505 (2014) 509–514.
[23] W. He, H. Wan, L. Hu, et al., Cell Res. 25 (2015) 1285–1298.
[24] S.L. Fink, B.T. Cookson, Cell. Microbiol. 8 (2006) 1812–1825.
[25] E.A. Miao, I.A. Leaf, P.M. Treuting, et al., Nat. Immunol. 11 (2010) 1136–1142.
[26] C. Rogers, D.A. Erkes, A. Nardone, et al., Nat. Commun. 10 (2019) 1689.
[27] Y.J. Ko, J.W. Lee, E.J. Yang, Biomaterials 226 (2020) 119543.
[28] J. Yu, S. Li, J. Qi, et al., Cell Death Dis. 10 (2019) 1–13.
[29] Y. Wang, W. Gao, X. Shi, et al., Nature 547 (2017) 99–103.
[30] C. Rogers, T. Fernandes-Alnemri, L. Mayes, et al., Nat. Commun. 8 (2017) 14128.
[31] X. Yang, G. Chen, K. Yu, et al., Cell Death Dis. 11 (2020) 295.
[32] Y. Wang, W. Gao, X. Shi, et al., Nature 547 (2017) 99–103.
[33] L. Hu, M. Chen, X. Chen, et al., Cell Death Dis. 11 (2020) 281.
[34] Y. Wang, J. Weng, X. Wen, et al., Biomater. Sci. (2020), doi:http://dx.doi.org/10.1039/D0BM00895H.
[35] R. Yan, D. Ye, Sci. Bull. 61 (2016) 1672–1679.
[36] M. Palner, B. Shen, J. Jeon, et al., J. Nucl. Med. 56 (2015) 1415–1421.
[37] L. Qiu, W. Wang, K. Li, et al., Theranostics 9 (2019) 6962–6975.
[38] Q. Nguyen, G. Smith, M. Glaser, et al., Proc. Natl. Acad. Sci. U. S. A. 106 (2009) 16375–16380.
[39] D. Ye, A.J. Shuhendler, P. Pandit, et al., Chem. Sci. 5 (2014) 3845–3852.
[40] H. Li, G. Parigi, C. Luchinat, et al., J. Am. Chem. Soc. 141 (2019) 6224–6233.
[41] Y. Yuan, H. Sun, S. Ge, et al., ACS Nano 9 (2015) 761–768.
[42] K. Akazawa, F. Sugihara, T. Nakamura, et al., Bioconjugate Chem. 29 (2018) 1720–1728.
[43] G. Liang, J. Ronald, Y. Chen, et al., Angew. Chem. Int. Ed. 50 (2011) 6283–6286.
[44] H. Nejadnik, D. Ye, O.D. Lenkov, et al., ACS Nano 9 (2015) 1150–1160.
[45] M. Zheng, Y. Wang, H. Shi, et al., ACS Nano 10 (2016) 10075–10085.
[46] M. Rehm, H. Düßmann, R.U. Jänicke, et al., J. Biol. Chem. 277 (2002) 24506–24514.
[47] H. Wang, Q. Zhang, X. Chu, et al., Angew. Chem. Int. Ed. 50 (2011) 7065–7069.
[48] J.V. Frangioni, Curr. Opin. Chem. Biol. 7 (2003) 626–634.
[49] K. Boeneman, B.C. Mei, A.M. Dennis, et al., J. Am. Chem. Soc. 131 (2009) 3828–3829.
[50] H. Liu, L. Chen, C. Xu, Chem. Soc. Rev. 47 (2018) 7140–7180.
[51] C. Yang, Q. Wang, W. Ding, RSC Adv. 9 (2019) 25285–25302.
[52] L. Tyas, V.A. Brophy, A. Pope, et al., Eur. Mol. Biol. Org. Rep. 1 (2000) 266–270.
[53] K. Kim, M. Lee, H. Park, et al., J. Am. Chem. Soc. 128 (2006) 3490–3491.
[54] E.A. Jares-Erijman, T.M. Jovin, Nat. Biotechnol. 21 (2003) 1387–1395.
[55] K. Bullok, D. Piwnica-Worms, J. Med. Chem. 48 (2005) 5404–5407.
[56] K.E. Bullok, D. Maxwell, A.H. Kesarwala, et al., Biochemistry 46 (2007) 4055–4065.
[57] E.M. Barnett, X. Zhang, D. Maxwell, et al., Proc. Natl. Acad. Sci. U. S. A. 106 (2009) 9391–9396.
[58] D. Maxwell, Q. Chang, X. Zhang, et al., Bioconjugate Chem. 20 (2009) 702–709.
[59] G. Leriche, G. Budin, Z. Darwich, et al., Chem. Commun. 48 (2012) 3224–3226.
[60] W. Tao, N. Kong, X. Ji, et al., Chem. Soc. Rev. 48 (2019) 2891–2912.
[61] X. Wang, J. Sheng, M. Yang, Chin. Chem. Lett. 30 (2019) 533–540.
[62] X. Huang, S. Lee, X. Chen, Am. J. Nucl. Med. Mol. Imaging 1 (2011) 3–17.
[63] S. Lee, K.Y. Choi, H. Chung, et al., Bioconjugate Chem. 22 (2011) 125–131.
[64] Y. Liu, Y. Hu, Y. Guo, et al., J. Control. Release 163 (2012) 203–210.
[65] D.J. Maxwell, J.R. Taylor, S. Nie, J. Am. Chem. Soc. 124 (2002) 9606–9612.
[66] G. Chen, I. Roy, C. Yang, et al., Chem. Rev. 116 (2016) 2826–2885.
[67] S. Zhang, X. Pei, H. Gao, et al., Chin. Chem. Lett. 31 (2020) 1060–1070.
[68] W. Gao, L. Ji, L. Li, et al., Biomaterials 33 (2012) 3710–3718.
[69] Q. Wang, W. Hu, Q. Feng, et al., RSC Adv. 5 (2015) 43824–43830.
[70] Q. Li, X. Qiao, F. Wang, et al., Anal. Chem. 91 (2019) 13633–13638.
[71] Z.R. Grabowski, K. Rotkiewicz, W. Rettig, Chem. Rev. 103 (2003) 3899–4031.
[72] B. Valeur, I. Leray, Coord. Chem. Rev. 205 (2000) 3–40.
[73] Y. Wu, W. Zhu, Chem. Soc. Rev. 42 (2013) 2039–2058.
[74] J. Huang, J. Li, Y. Lyu, et al., Nat. Mater. 18 (2019) 1133–1143.
[75] J. Luo, Z. Xie, J.W.Y. Lam, et al., Chem. Commun. (2001) 1740–1741.
[76] H. Wang, E. Zhao, J.W.Y. Lam, et al., Mater. Today 18 (2015) 365–377.
[77] H. Shi, R.T.K. Kwok, J. Liu, et al., J. Am. Chem. Soc. 134 (2012) 17972–17981.
[78] H. Shi, N. Zhao, D. Ding, et al., Org. Biomol. Chem. 11 (2013) 7289–7296.
[79] D. Ding, J. Liang, H.B. Shi, et al., J. Mater. Chem. B 2 (2014) 231–238.
[80] A. Han, H. Wang, R.T.K. Kwok, et al., Anal. Chem. 88 (2016) 3872–3878.
[81] Y. Yuan, R. Zhang, X. Cheng, et al., Chem. Sci. 7 (2016) 4245–4250.
[82] H. Li, G. Parigi, C. Luchinat, et al., J. Am. Chem. Soc. 141 (2019) 6224–6233.
[83] Y. Yuan, R.T.K. Kwok, B. Tang, et al., J. Am. Chem. Soc. 136 (2014) 2546–2554.
[84] K. Zhang, Y. Gao, P. Yang, et al., Adv. Healthc. Mater. 7 (2018) 1800344.
[85] Y. Li, H. Zhou, J. Chen, et al., Biosens. Bioelectron. 76 (2016) 38–53.
[86] A. Razgulin, N. Ma, J. Rao, Chem. Soc. Rev. 40 (2011) 4186–4216.
[87] Y. Cui, W. Du, G. Liang, Chem. Nano. Mat. 2 (2016) 344–353.
[88] R. Huang, X. Wang, D. Wang, et al., Anal. Chem. 85 (2013) 6203–6207.
[89] D. Ye, A.J. Shuhendler, L. Cui, et al., Nat. Chem. 6 (2014) 519–526.
[90] Y. Wang, X. Hu, J. Weng, et al., Angew. Chem. Int. Ed. 131 (2019) 4940–4944.
[91] Z. Chen, M. Chen, Y. Cheng, et al., Angew. Chem. Int. Ed. 59 (2020) 3298–3305.
[92] Z. Chen, M. Chen, K. Zhou, et al., Angew. Chem. Int. Ed. 59 (2020) 7864–7870.
[93] E.I. Deryugina, B. Ratnikov, E. Monosov, et al., Exp. Cell Res. 263 (2001) 209–223.
[94] R. Lebel, M. Lepage, Contrast Media Mol. Imag. 9 (2014) 187–210.
[95] M.W. Roomi, J.C. Monterrey, T. Kalinovsky, et al., Oncol. Rep. 21 (2009) 1323–1333.
[96] A. Rotte, M. Martinka, G. Li, Cell Oncol. 35 (2012) 207–216.
[97] X. Liang, R. Sun, X. Zhao, et al., J. Cell. Mol. Med. 21 (2017) 3579–3591.
[98] J. Lida, K.L. Wilhelmson, J. Ng, et al., Biochem. J. 403 (2007) 553–563.
[99] J.M. Pellikainen, K.M. Ropponen, V.V. Kataja, et al., Clin. Cancer Res. 10 (2004) 7621.
[100] S. Li, L. Liu, H. Cheng, et al., Chem. Commun. 51 (2015) 14520–14523.
[101] H. Cheng, S. Li, H. Zheng, et al., Anal. Chem. 89 (2017) 4349–4354.
[102] Y. Yuan, C. Zhang, R.T.K. Kwok, et al., Chem. Sci. 8 (2017) 2723–2728.
[103] Y. Wen, K. Liu, H. Yang, et al., Anal. Chem. 86 (2014) 9970–9976.
[104] Y. Wen, F. Xue, H. Lan, et al., Biosens. Bioelectron. 91 (2017) 115–121.
[105] K. Heinzmann, L.M. Carter, J.S. Lewis, et al., Nat. Biomed. Eng. 1 (2017) 697–713.
[106] Y. Fan, P. Wang, Y. Lu, et al., Nat. Nanotechnol. 13 (2018) 941–946.
[107] P. Cheng, Q. Miao, J. Li, et al., J. Am. Chem. Soc. 141 (2019) 10581–10584.